Agglomeration in a Continuous MSMPR Crystallizer

Narayan S. Tavare and Anand V. Patwardhan
Dept. of Chemical Engineering, University of Manchester Institute of Science and Technology (UMIST), Manchester M60 1QD, England

Experimental responses from crystallization of copper sulfate pentahydrate, nickel ammonium sulfate, potassium sulfate, and soy protein in continuous MSMPR crystallizers were used to determine simultaneously crystal growth and nucleation rates and agglomeration kernels. Measured product crystal size distributions at steady state for all these systems were transformed into crystal volume coordinates to use two methods: moments analysis and optimization procedure for parameter characterization. An iterative nonlinear parameter estimation by optimization procedure was used to deduce the kinetic rate parameters in the solution of the agglomeration model in crystal volume coordinates, extended from the analysis by Liao and Hulburt (1976), from the translated data set for the product crystals. The kinetic results obtained for the copper sulfate pentahydrate system were correlated in terms of power law kinetic expressions depicting the effect of significant observable variables.

Introduction

As the presence of agglomerated particles in crystallizing systems is fairly common, considerable attention has been paid in many recent studies dealing with agglomeration of crystals during precipitation (or crystallization) in understanding the factors that contribute to their formation and to the development of theories to account for their characterization (see, for example, Table 4 of Tavare, 1986). Hartel et al. (1986) studied the tendency for aggregation and disruption of aggregates of calcium oxalate dihydrate crystals in urine-like mother liquor in a two-stage MSMPR (mixed suspension mixed product removal) crystallizer and Couette flow aggregator operated in series. To model the experimental crystal size distribution, Hartel and Randolph (1986) developed a numerical algorithm to solve the population balance equation that included the aggregation and rupture terms and used both the experimental and numerical solutions to formulate the aggregation and disruption functions.

Franck et al. (1988) investigated the kinetics of salicylic acid precipitation from sodium salicylate and sulfuric acid in a batch crystallizer by conductometry, and the final product size was determined from a population balance model incorporating primary and secondary nucleation, chemical- and diffusion-controlled growth and agglomeration of crystals. David et al. (1991a) developed a discrete formulation of the agglomeration rate of adipic acid crystals during crystallization in mechanically stirred crystallizer. The expression relied on fluid mechanics and phenomenological considerations, and accounted for the influence of particle concentration, supersaturation, specific power dissipation, size of crystallizer and size of agglomerating crystals. An algorithm for process identification and simulation analysis was developed for a semibatch crystallization of adipic acid, measured conductivity of solutions and crystal size distributions as a function of time being used as experimental responses. A complete kinetic model involving nucleation, growth and agglomeration processes and eight kinetic parameters was proposed by David et al. (1991b) the method of isolation being considered to fit four parameters at a time by optimization as different kinetic processes controlled the successive steps of crystallization.

Przybycien and Bailey (1989) investigated environmental factors affecting perikinetics aggregation induced by salt addition in the case of α-chymotrypsin. Stopped flow turbidimetry and dynamic laser scattering were used to monitor the progress of precipitation process. A detailed population balance model specifically for proteins with quaternary interactions was proposed to account for specific and nonspecific

Correspondence concerning this article should be addressed to N. S. Tavare.
Present address of A. V. Patwardhan: Department of Chemical Engineering, University of Nottingham, University Park, Nottingham NG7 2RD, England.

interactions and monomer addition. Zumstein and Rousseau (1989a) studied agglomeration of copper sulfate pentahydrate in batch, semibatch and continuous crystallizers. The percentage of agglomerates as determined from volume shape factors depended on the actual level of supersaturation prevailing in the vessel. Masy and Cournil (1991) used turbidimetry to characterize the kinetics of agglomeration of a finely ground sample of potassium sulfate having size in the region of ~ 1 μm in different stirred media. When the particles agglomerated, their contribution to the global turbidity decreased. This information was used to determine the kinetics in purely agglomerating system.

The purpose of this article was to develop a technique that may be used to deduce simultaneously the kinetic rates for crystal growth, nucleation and agglomeration in an agglomerating system. The study was confined to the case of an experimental response obtained at steady state from an MSMPR crystallizer. Conventional product size distribution data obtained from a size analysis technique were transformed into product crystal volume distribution data. The agglomeration model suggested by Liao and Hulburt (1976) in crystal size coordinates was extended in crystal volume coordinates. The conservation of the crystal volume, rather than the crystal size as assumed previously, would thereby be preserved.

Theory

Population balance

Most precipitation processes usually result in agglomerated product. Agglomeration processes can be represented in the population balance by birth and death functions formulated on the basis of empirical description and also preserving the internal consistency. Although the precise mechanisms of agglomeration processes are difficult to conceive, a simple mechanism based on two body collisions has generally been used in formulating the rate models (see, for example, Table 4, Tavare, 1986). The agglomeration model proposed by Liao and Hulburt (1976) used characteristic length as an additive property and provided an analytical solution for a continuous MSMPR crystallizer. Randolph and Hartel (1986) presented their formulation in terms of crystal volume coordinates, rather than the crystal size, to incorporate aggregation and rupture terms in their numerical modeling of calcium oxalate aggregation behavior. Semi-empirical formulations for the aggregation and disruption functions were found that resulted in excellent matches between experimental and predicted conventional size domain distributions. Delpech de Saint Guilhem and Ring (1987) attempted an exact solution to the population balance equation in a continuous stirred tank solution in the crystal size domain. The exact solution had different functional form and characteristic points than those reported previously (Lamey and Ring, 1986). Hounslow et al. (1988) and Hounslow (1990a, b) in their numerical discretization scheme used classical population balance approach in crystal size coordinates transforming the conventional birth and death functions expressed in terms of crystal volume as the internal coordinate to the length-based form. In this study, crystal volume coordinates will be used throughout.

For an MSMPR crystallizer, the population balance equation in volume coordinates is:

$$G\frac{dn}{dv}+\frac{n}{\tau}=B-D \tag{1}$$

where G is the crystal-volume-independent overall growth rate (m^3/s) and n is crystal population density function expressed as a function of crystal volume (no./$m^3\cdot$L). B and D represent the empirical birth and death functions over a volume v and $v + dv$ such that $(B - D)dv$ represents the net appearance of particles most probably by aggregation mechanism between v and $v + dv$. The aggregation of two particles of volume u and $v - u$ into a particle volume v can be represented by the following birth and death functions for the present case as:

$$B_a=\frac{1}{2}\int_0^v \beta(u,v-u)n(u,t)n(v-u)du \tag{2}$$

and

$$D_a=n(v)\int_0^\infty \beta(u,v)n(u)du \tag{3}$$

The agglomeration kernel $\beta(u,v-u)$ is a measure of the frequency of collisions between particles of volumes u and $v-u$ that are successful in producing a particle of volume v. The factor 1/2 in Eq. 2 ensures that collisions are not counted twice. The agglomeration kernel $\beta(u,v-u)$ depends on the environment and accounts for the physical forces that are instrumental in the mechanism of aggregation, which decides its functional form. Although many theoretical and empirical formulations of agglomeration kernel are available (see, for example, Drake, 1972; Hartel and Randolph, 1986; Hounslow et al., 1988) to describe various mechanisms of aggregation, it may be necessary to assume that the agglomeration kernel is crystal-volume-independent, at least over a small range of experimental conditions used for the parameter identification of dynamic processes.

For an MSMPR crystallizer, the pertinent boundary condition to the population balance equation (Eq. 1) is:

$$n(0)=n^0=B_0/G \tag{4}$$

where B_0 is the nucleation rate of a precipitate at near zero crystal volume. Equation 4 suggests that the particle flux of newly generated crystals added to the particulate system is at a vanishingly small volume very close to zero.

Moment transformation

Following the treatment by Hulburt and Katz (1964), the moment transformation of the population balance equation (Eq. 1) (in crystal-volume coordinate) with respect to crystal volume, that is, multiplying by v^j and integrating each term of Eq. 1 with respect to v over the entire volume range $(0-\infty)$, yields a set of algebraic equations in μ_j as:

$$G[nv^j|_0^\infty - j\mu_{j-1}]+\frac{\mu_j}{\tau}=\beta\left[\frac{1}{2}\left(\sum_{k=0}^{j}\binom{j}{k}\mu_k\mu_{j-k}\right)-\mu_0\mu_j\right] \tag{5}$$

where $\binom{j}{k}$ is the binomial coefficient:

$$\binom{j}{k} = \frac{j!}{k!(j-k)!} \tag{6}$$

Moment equations for the first three moments (up to second-order) from Eq. 5 are:

$$-B_0 + \frac{\mu_0}{\tau} = -\frac{1}{2}\beta\mu_0^2 \tag{7}$$

$$\frac{\mu_1}{\tau} = G\mu_0 \tag{8}$$

$$\frac{\mu_2}{\tau} = 2G\mu_1 + \beta\mu_1^2 \tag{9}$$

Crystallization and agglomeration kinetics

To characterize the apparent rates associated with the evolution of the particulate system during the precipitation processes, several techniques have been reported in the crystallization literature. The rate processes required to characterize in a commercial precipitation vessel are crystal growth, nucleation and agglomeration, and can be characterized by the simple method of moments analysis. The experimentally determined population data at steady state can be converted into the moments with respect to crystal volume using the definition of moments as:

$$\mu_j = \int_0^\infty n(v)v^j dv \tag{10}$$

These moments of experimentally measured population density data can be used to determine rates of the processes as:

$$G = \frac{\mu_1}{\mu_0\tau} \tag{11}$$

$$\beta = \frac{1}{\mu_1^2}\left[\frac{\mu_2}{\tau} - 2G\mu_1\right] = \frac{1}{\tau}\left[\frac{\mu_2}{\mu_1^2} - \frac{2}{\mu_0}\right] \tag{12}$$

and

$$B_0 = \frac{\mu_0}{\tau} + \frac{1}{2}\beta\mu_0^2 = \frac{\mu_2\mu_0^2}{2\tau\mu_1^2} \tag{13}$$

These three relations are derived from the moment equations (Eqs. 7-9) and can be used to determine the rates from the moments of experimental population density data obtained during the course of an MSMPR experiment at steady state.

It is also possible to derive the analytical solution to Eq. 1. To present the solution in a simple analytical expression, if the following dimensionless variables (see, for example, Liao and Hulburt, 1976) can be defined as:

$$f(x) = \frac{n}{n^0} = \frac{nG}{B_0} \quad x = \frac{v}{G}\sqrt{2\beta B_0} \quad P = \sqrt{1 + \frac{1}{2\beta B_0\tau^2}} \tag{14}$$

Equation 1 then can be modified in terms of the dimensionless population balance equation to:

$$\frac{df(x)}{dx} + Pf(x) = \frac{1}{4}\int_0^x f(x-x')f(x')dx' \tag{15}$$

with the boundary condition:

$$f(0) = 1 \tag{16}$$

Solution to Eq. 15 by the Laplace transform technique using the negative square root as a physically meaningful solution can be obtained as:

$$f(x) = 2\exp(-\mathrm{Px})\frac{I_1(x)}{x} \tag{17}$$

where $I_1(x)$ is the first-order modified Bessel function of the first kind. The cumulative overvolume number distribution of crystals can be obtained from Eq. 17 as:

$$\eta = \sqrt{\frac{2B_0}{\beta}}\int_x^\infty \exp(-Px)\frac{I_1(x)}{x}dx \tag{18}$$

This analytical solution as suggested by Liao and Hulburt (1976) can be used to analyze experimental data from an MSMPR crystallizer and to estimate simultaneously the rates of the kinetic processes. The Laplace transform domain techniques can also be used as Eq. 15 can be transformed into the Laplace domain.

Crystal growth and nucleation rates and agglomeration kernel obtained from a series of experimental runs can be correlated by empirical kinetic relations in terms of most significant and observable variables. In the present study, the applicable power law kinetic correlations for the copper sulfate pentahydrate—water system are:

$$G = k_g\sigma^g \tag{19}$$

$$B_0 = K_R G^i M_T^j \tag{20}$$

and

$$\beta = k_\beta G^h B_0^p \tau^q \tag{21}$$

The rate coefficients k_g, K_R, and k_β are empirical constants accounting for other significant variables.

Experimental Studies

Previously published experimental results of product size distributions from a steady-state continuous MSMPR crystallizer for four systems were used to characterize the kinetic rates using the present theoretical development, the relevant details being shown in Table 1. For full experimental details original references should be consulted. Both sieve and Coulter counter analyses were used for the size analysis of nickel ammonium sulfate and potassium sulfate crystals, and only Coulter counter analysis for soy protein and sieve analysis for copper sulfate pentahydrate were used. Experimental sieve analysis results from a series of 14 experiments for copper sulfate pentahydrate crystals were used in detail for analytical treatment, while only one or two illustrative size analysis results for the

Table 1. Experimental Systems Used in This Study

System	Crystallizer	Mode	Temp. °C	Authors
Copper sulfate pentahydrate	13-L MSMPR	Cooling	26.7	Zumstein and Rousseau (1989)
Nickel ammonium sulfate	5-L MSMPR	Reaction	25	Tavare et al. (1985)
Potassium sulfate	8-L MSMPR	Vacuum	30	Rosen and Hulburt (1971)
Soy protein	2-L MSMPR	Reaction	25	Grabenbauer and Glatz (1981)

other systems, as reported in the literature, are considered. In the case of MSMPR crystallization of copper sulfate pentahydrate from aqueous solution of industrial grade salt two-four samples were taken from the suspension after ten residence times for the sieve analysis. The magma density was determined for each sample, and the residence time in the crystallizer for each run was determined from a material balance. Relative supersaturation was defined as the ratio of liquor concentration to the saturation concentration, both of which are expressed in kg copper sulfate pentahydrate/kg water. Although most experiments were performed with a residence time of about 1,800 s, the range of magma concentration, residence time, stirrer speed and relative supersaturation were 0.03-0.2 kg/L, 1,800-5,400 s, 16.7-25.0 rev/s, and 0.029-0.057, respectively.

Results and Discussion

Population density as a function of crystal volume can be determined from the sieve analysis. For a specific case, for example, with the material retained w between two adjacent sieve sizes differing by ΔL (equivalent Δv) and having mean size L (or volume $v = k_v L^3$) with magma concentration M_T within the crystallizer the population density (expressed as no/m^3·L) at crystal volume v can be determined by:

$$n = \frac{wM_T}{\rho_c v \Delta v \Sigma w} \tag{22}$$

Results of population density calculations for copper sulfate pentahydrate crystals obtained from three-four samples for each run during three runs with different residence times (~ 1,800, 3,600 and 5,400 s) at a stirrer speed of 25 rev/s are shown in Figure 1 as a population density plot (ln n against v on a logarithmic scale). Conventional population density plots (ln n vs. L) in size coordinates for this system (as shown in Figure 6 of Zumstein and Rousseau, 1989a, for Run 3.5 with τ ~ 5,400 s) show upward curvature at smaller size, indicating a deviation from the assumptions inherent in the development of a simple exponential relation. The authors attributed this deviation to the combination of growth abnormalities (that is, size-dependent growth and/or growth dispersion) and agglomeration. The population density plots evaluated by Liao and Hulburt (1976) using their simplified analytical solution to an agglomeration model also show similar upward curvature. The data for the three runs in Figure 1, however, show the different (convex downward) curvature at large size. The population density data in volume coordinates for the illustrative runs of the other three systems in Figure 2 also indicate similar variations. All the conventional population density plots in size coordinates as depicted in the original references show upward concave curvature at lower size.

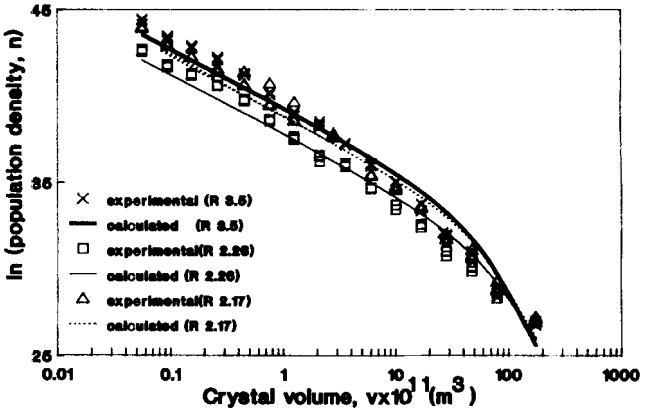

Figure 1. Population density data for copper sulfate pentahydrate crystals (Zumstein and Rousseau, 1989a).

All these population density data in crystal volume coordinates obtained from the product size distributions were used to calculate numerically the moments with respect to crystal volume up to second-order using Eq. 10. The calculated moments were then used to determine the crystal volume growth (Eq. 11), apparent nucleation rate (Eq. 13), and agglomeration kernel (Eq. 12). The results for the data in Figures 1-2 and also for other runs are reported in Table 2. The best estimates of kinetic parameters (G, B_0 and β) in Eqs. 14 and 15 were also determined from the experimental population density—crystal volume data as in Figures 1-2 using a comprehensive iterative algorithm for the solution of nonlinear least squares problem available as a computer library subroutine (program E04FCF in NAG library). The algorithm finds an unconstrained minimum of sum of squares of objective function involving a set of nonlinear equations in several variables without requiring separate evaluations of any derivatives. The objective function chosen was the logarithmic difference between the experimental and predicted population density defined in crystal-volume coordinates.

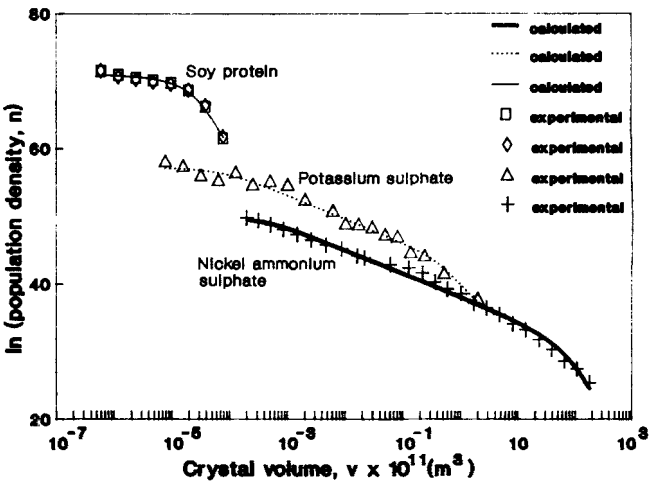

Figure 2. Population density data for three systems.

Table 2. Parameter Estimates in the Volume Coordinates

Technique		$B_0\times10^{-6}$ no./L·s	$G\times10^{17}$ m³/s	$\beta\times10^{11}$ L/no.·s	$B_0/G\times10^{-22}$ no./m³·L	Σe^2	m
Copper sulfate pentahydrate (Zumstein and Rousseau, 1989)							
Run 2.26	$\tau=1{,}764$ s	$M_T=0.036$ kg/L		$N=25.0$ rev/s		$\sigma=0.0563$	
Moments analysis		0.08	286	191	2.8×10^{-3}	34.8	48
LSQNDN algorithm		0.14	204	385	6.8×10^{-3}	21.9	48
Run 2.17	$\tau=3{,}564$ s	$M_T=0.098$ kg/L		$N=25.0$ rev/s		$\sigma=0.0380$	
Moments analysis		0.105	118.1	26.0	8.9×10^{-3}	48.7	45
LSQNDN algorithm		0.163	94.9	60.6	1.7×10^{-2}	16.3	45
Run 3.5	$\tau=5{,}394$ s	$M_T=0.141$ kg/L		$N=25.0$ rev/s		$\sigma=0.0291$	
Moments analysis		0.10	74.1	5.5	1.4×10^{-2}	185	64
LSQNDN algorithm		0.20	50.4	23.9	4.0×10^{-2}	43.7	64
Nickel ammonium sulfate (Run B23, Tavare et al., 1985)							
$\tau=900$ s		$M_T=0.091$ kg/L		$N=20$ rev/s		$\Delta c=0.0072$ kg/kg	
Moments analysis		2.2	102	279	0.21	30.0	26
LSQNDN algorithm		4.9	89.6	469	0.54	9.0	26
Potassium sulfate (Run 1, Rosen and Hulburt, 1971)							
$\tau=2{,}909$ s		$M_T=0.063$ kg/L		$N=16.7$ rev/s		$\Delta c=0.00041$ kg/kg	
Moments analysis		176	0.92	0.12	1,900	18.0	19
LSQNDN algorithm		106	1.42	0.17	740	12.0	19
Soy protein (Runs 4 and 5, Grabenbauer and Glatz, 1981)							
$\tau=800$ s		$M_T=-0.108$ kg/L		$N=3.75$ rev/s		$c_f=-0.019$ kg/L	
Moments analysis		1.5×10^{6}	0.011	0.2×10^{-8}	1.4×10^{9}	153	16
LSQNDN algorithm		7.6×10^{4}	0.010	0.3×10^{-7}	7.4×10^{7}	1.5	16

A logarithmic sum of squares was employed since there was several orders of magnitude difference in population density between the smallest and largest crystals. This allowed the whole distribution to be accounted for with equal accuracy. The step length or improvement vector in an iterative sequence is usually chosen such that the sum of squares at the subsequent iteration is approximately a minimum with respect to the step length vector. The directional vector normally depends on the reduction in sum of squares obtained during the last iteration. The computer program was designed to ensure that the steady progress was achieved whatever the starting point and to have a rapid ultimate convergence. The number of iterations required depended on the number of parameters, the number of observations, the behavior of the objective function, the accuracy demanded, and the distance of the starting point from the solution. In the present case, both the independent variable (crystal volume) and the parameters (G, B_0 and β) were scaled so that they were each around unity. This would imply that the Hessian matrix near solution was well conditioned. In the present study, the parameter estimates determined from the moment analysis (Eqs. 11-13) were used as initial guesses, which provided an efficient convergence in all the cases. The best parameter estimates were selected using the minimum possible sum of residual squares through several trials. The results so obtained for the data in Figures 1 and 2 are also included in Table 2. Both techniques, moments analysis and optimization procedure, appear to yield reasonable results, and the optimization procedure gives potentially better accuracy. In most cases, both nucleation rates and agglomeration kernels estimated by the optimization routine are higher, and growth rates are lower than the corresponding estimates obtained from the moments analysis. The curves in Figures 1 and 2 resulted from smooth curve fitting obtained through the data points calculated from the analytical solution (Eqs. 14-15) using the parameter estimates determined by the optimization procedure.

The population density data in crystal size coordinates corresponding to the data in crystal volume coordinates in Figures 1 and 2 were reported in the original work (Table 1) and used to determine kinetic parameters by the moments analysis in crystal-size coordinates. The analytical equations for the moments are identical except that the moments with respect to size are determined from the original data in the size coordinates system. Table 3 shows kinetic parameter estimates as well as the results obtained from the iterative nonlinear parameter estimation library subroutine for the data in crystal-size coordinates using previously reported analytical solution to the population balance equation in crystal-size coordinates (Liao and Hulburt, 1976; Tavare et al., 1985). The analytical solutions used are again identical and can be obtained replacing v by L in the present development. In most cases, the moments analysis appears to yield negative values of agglomeration kernel. Reasonable values of kinetic parameters estimates were obtained from the optimization subroutine. Generally higher values of nucleation rates and lower values of growth rates were obtained by implementing the optimization routine than by moment analysis.

Values of both the nucleation rate and agglomeration kernel in volume coordinates are numerically higher than those in size coordinates as determined by the optimization procedure in both cases. Parameter estimates determined by the present library subroutine in crystal-size coordinates for both nickel ammonium sulfate and potassium sulfate are consistent with previously reported values using the Marquardt algorithm [for nickel ammonium sulfate, $G' = 0.036$ μm/s, $B_0' = 0.18\times10^{6}$ no./L·s, $\beta' = 2.5\times10^{-11}$ L/no.·s, Tavare et al. (1985) and Tavare (1991); for potassium sulfate, $G' \sim 0.001 - 0.006$ μm/s, $B_0' \sim 0.15\times10^{6} - 6\times10^{6}$ no./L·s, $\beta' \sim 2\times10^{-15} -$

Table 3. Parameter Estimates in the Size Coordinates

Technique		$B_0' \times 10^{-6}$ no./L·s	$G' \times 10^{8}$ m/s	$\beta' \times 10^{12}$ L/no.·s	$\eta_0' \times 10^{-13}$ no./m·L	Σe^2	m
Copper sulfate pentahydrate (Zumstein and Rousseau, 1989)							
Run 2.26	$\tau = 1{,}764$ s		$N = 25.0$ rev/s			$\sigma = 0.0563$	
Moments analysis		0.003	7.2	−45.2	0.04		
LSQNDN algorithm		0.013	2.2	39.9	0.61	7.3	48
Run 2.17	$\tau = 3{,}564$ s		$N = 25.0$ rev/s			$\sigma = 0.380$	
Moments analysis		0.005	3.4	−7.4	0.014		
LSQNDN algorithm		0.036	0.8	5.6	0.45	5.3	45
Run 3.5	$\tau = 5{,}394$ s		$N = 25.0$ rev/s			$\sigma = 0.0291$	
Moments analysis		0.007	2.3	−2.4	0.3		
LSQNDN algorithm		0.04	0.49	1.8	8.9	6.1	64
Nickel ammonium sulfate (Run B23, Tavare et al., 1985)							
Moments analysis		0.05	6.6	4.7	0.07	35	26
LSQNDN algorithm		0.42	2.1	29.8	2.0	1.8	26
Potassium sulfate (Run 1, Rosen and Hulburt, 1971)							
Moments analysis		4.54	0.8	0.009	57.7	13.	19
LSQNDN algorithm		6.68	0.6	0.008	111	8.4	19
Soy protein (Runs 4 and 5, Grabenbauer and Glatz, 1981)							
Moments analysis		0.85×10^{6}	0.61	-0.9×10^{-6}	1.4×10^{7}		
LSQNDN algorithm		0.66×10^{6}	0.52	0.5×10^{-20}	1.2×10^{7}	42	16

2×10^{-12} L/no.·s, Liao and Hulburt (1976)]. The present results of crystal-volume growth rate and crystal-size growth rate are consistent with one another. The crystal-size growth determined from the agglomeration models are usually lower than that by growth experiments (Liao and Hulburt, 1976; Tavare et al., 1985). Tables 2-3 indicate that both copper sulfate and nickel ammonium sulfate tend to form agglomerate particularly at the high level of supersaturation. Both potassium sulfate and soy protein appear to form fewer agglomerates as indicated by lower values of agglomeration kernel (β or β'). Crystal breakage is important in the case of soy protein, resulting in very low values of agglomeration kernel.

Kinetic correlations

All the growth and and nucleation rates and agglomeration kernels obtained for the copper sulfate pentahydrate system in 14 runs were correlated with empirical power law expressions (Eqs. 19-21). Only a few supersaturation measurements were available. The crystal-volume growth rates were correlated using a linear least squares technique by Eq. 19, as shown in Figure 3. The regression correlation coefficient for the data excluding one point in Figure 3 is 0.98. The growth rate order with respect to the relative supersaturation is well within the range of previously reported values ranging from 1.2 to 2.6 (see, for example, Table II, Zumstein and Rousseau, 1989b). Growth rates predicted by this correlation appear to have significant contribution from surface integration step.

Nucleation kinetics for MSMPR experiments are usually correlated empirically by an expression in Eq. 20. Parameter estimates obtained by multiple linear regression analysis of all the nucleation rate data gave the correlation in Figure 4. Both the exponents (i and j) are estimated with a reasonable confidence ($\sigma_i^2 = 0.066$ and $\sigma_j^2 = 0.053$), and the root mean relative error based on the observed value for the correlation is ~ 5%. A near-unity exponent of magma density in the relative nucleation kinetics (eq. 20) indicates the possibility of dominance of secondary nucleation mechanism. A negative kinetic order is probably the characteristics of size-limiting nucleation phe-

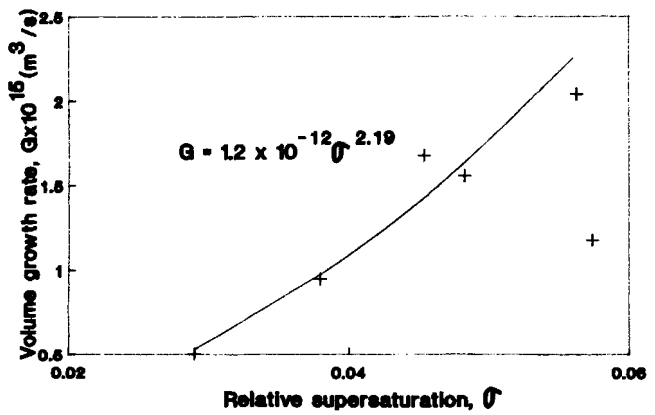

Figure 3. Growth rate correlation.

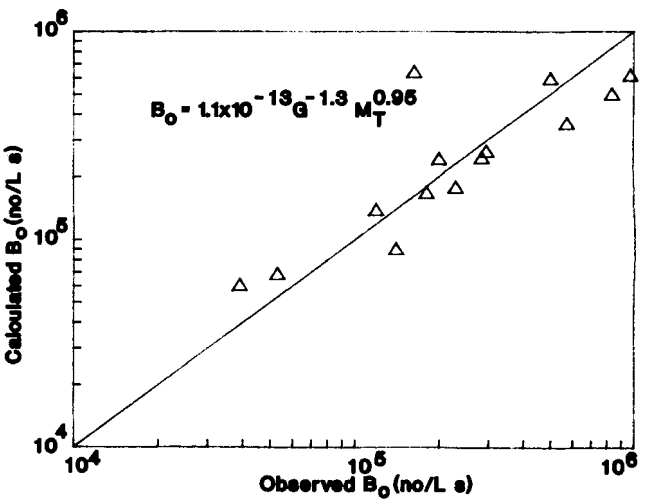

Figure 4. Relative nucleation rate correlation.

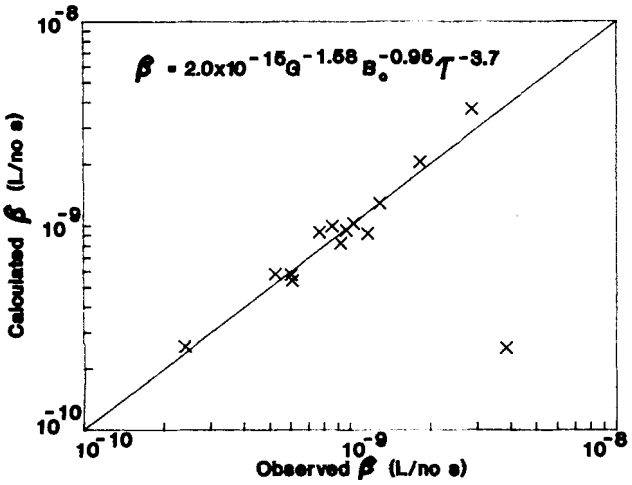

Figure 5. Correlation for agglomeration kernel.

nomena in MSMPR studies as described by Randolph and Cise (1972) and Youngquist and Randolph (1972) (see also, Zumstein and Rousseau, 1989b).

Agglomeration kernels obtained in all the experiments were correlated by the empirical power law relationship (Eq. 21) as shown in Figure 5. All the exponents (h, p, q) were estimated with a reasonable confidence ($\sigma_h^2=0.04$, $\sigma_p^2=0.01$, $\sigma_q^2=0.12$) and the root mean square relative error based on the observed value is ~ 1%. In this correlating equation (Eq. 21), the crystal-volume growth rate can be taken as the measure of the solution supersaturation, the nucleation rate or the particle flux at zero crystal volume B_0 provides a total rate measure of newly generated particle, and the mean residence time provides a measure of probability of particle stay within an MSMPR crystallizer. Thus, the products of $G\tau$ and $B_0\tau$ provide mean crystal volume of a particle from the slurry and crystal number concentration of newly generated particles in the crystallizer. Both magma concentration and stirrer speed showed less significance in the correlation for agglomeration kernel over the small range of variables used during the experimental program for the copper sulfate pentahydrate-water system. Indirectly through the nucleation rate, however, the magma concentration showed negative effect perhaps indicating that increasingly frequent and energetic collisions at high solid concentrations had a dominant effect in breaking down the agglomerates. The correlation for the agglomeration kernel indicates that the relative supersaturation through the values of G and B_0 appears to have less significant overall influence. The relative supersaturation was changed by changing the mean residence time of the crystallizer, most experiments being carried out with $\tau \sim 1{,}800$ s resulting in values of σ ranging from 0.045 to 0.065. The percentage of agglomerates as defined in terms of the volume shape factors of actual, well formed crystals and agglomerates appeared to depend on the level of supersaturation and crystal size, but have no noticeable effect of magma density and agitation (Zumstein and Rousseau, 1989a). Their batch crystallization studies indicated the importance of not only the level of supersaturation but also the time of exposure to the prevailing level of supersaturation.

The agglomeration model originally proposed by Liao and Hulburt (1976) considered the formation of agglomerates due to two-particle collision and assumed a characteristic length used as the parameter characterizing the size of agglomerating crystal as an additive property. The characteristic linear size, however, is not a conserved property. In this study, crystal volume was used as a characteristic property, and similar analytical solution in terms of crystal volume to the population balance equation was obtained. A further assumption, in addition to those usually made for the MSMPR crystallizer, again made for the sake of simplicity, is that the collision frequency factor β does not depend on crystal volume. The accommodation factor, which essentially gives the probability that two colliding particles cohere to form an agglomerate, is absorbed in this collision frequency factor β. There are many formulations, both theoretical and empirical, for the aggregation kernel that describe various mechanisms of aggregation (Drake, 1972; Tavare et al., 1985; Hartel and Randolph, 1986). It is rather difficult to define a single mechanism by which agglomeration occurs in a system. Zumstein and Rousseau (1989a) speculated in the case of copper sulfate pentahydrate crystals that a considerable growth occurs when two crystals form an agglomerate causing areas of two crystals to overlap and hindering the growth of constituent crystals.

Conclusions

This work was concerned primarily with the characterization of both crystallization and agglomeration kinetics from a series of experimental runs performed in MSMPR crystallizers at steady state for four systems. Previously published experimental product crystal-size distribution data classified as a function of crystal size for copper sulfate pentahydrate, nickel ammonium sulfate, potassium sulfate, and soy protein were transformed as a function of crystal volume. Both methods, the method of moments analysis and that of iterative nonlinear parameter estimation by optimization routine, were used in crystal volume coordinates to determine crystal-volume growth rate, apparent nucleation rates depicting the particle flux at zero crystal volume and agglomeration kernel describing the effective collision frequency in the process of agglomerate formation.

Parameter estimates in volume coordinates for the four systems were compared with the corresponding results obtained from the analysis of the same experimental data in size coordinates. Kinetic correlations for these rate processes in terms of *observables*, such as relative supersaturation, magma concentration and residence time, were established from the kinetic results obtained by the optimization procedure for the copper sulfate pentahydrate—water system. Although it is clearly difficult to define a single mechanism by which the agglomeration occurs in a crystallizing system, the agglomeration of two crystals followed by a considerable crystal growth in the case of copper sulfate pentahydrate crystals was speculated by Zumstein and Rousseau (1989a). The present study explains the techniques and measurements required in a continuous MSMPR crystallizer as represented in crystal-volume coordinates to formalize the basis for an overall process identification in the agglomerating precipitation system.

Acknowledgment

The authors wish to thank Professor R. W. Rousseau, Director, Georgia Institute of Technology, Atlanta, who provided the original sieve analysis data for copper sulfate pentahydrate crystals.

Notation

B = birth rate function, no./m^3·L·s
B_a = birth rate function due to aggregation, no./m^3·L·s
B_0 = nucleation rate, no./L·s
c = concentration, kg hydrate/kg water, kg/L
Δc = supersaturation, kg salt/kg water
D = death rate function, no./m^3·L·s
D_a = death rate function due to aggregation, no./m^3·L·s
f = dimensionless crystal size distribution, n/n^0
g = exponent of relative supersaturation in growth rate correlation (Eq. 19)
G = overall crystal volume growth rate, m^3/s
G' = overall linear growth rate, m/s
h = exponent of growth rate in aggregation kernel correlation (Eq. 21)
i = relative nucleation kinetic order (Eq. 20)
$I_1(x)$ = modified Bessel function of the first kind of order one
j = exponent of magma density in nucleation rate correlation (Eq. 20)
j, k = index variables
k_a = surface shape factor
k_g = growth rate constant (Eq. 19), m^3/s
K_R = relative nucleation rate constant (Eq. 20), no./[L·s·(m^3/s)^i·(kg/L)^j]
k_v = volume shape factor
k_β = rate coefficient for agglomeration kernel (Eq. 21), L/[no·s·(m^3/s)^h·(no./L·s)$p(s)q$]
L = crystal size, m, μm
m = number of data points used for analysis
M_T = magma density, kg/L
n = crystal volume population density, no./m^3·L
n' = crystal size population density, no./m·L
n^0 = nuclei population density, B_0/G, no./m^3·L
n'^0 = nuclei population density, B_0'/G', no./m·L
N = stirrer speed, rev/s
p = exponent of nucleation rate in agglomeration correlation (Eq. 21)
P = dimensionless parameter (Eq. 14)
q = exponent of mean residence time in agglomeration correlation (Eq. 21)
t = time, s
u = dummy variable for crystal volume, m^3
v = crystal volume, m^3, μm^3
w = weight, kg
x = dimensionless crystal size (Eq. 14)

Greek letters

β = agglomeration kernel in volume coordinates, L/no.·s
β' = agglomeration kernel in size coordinates, L/no.·s
Δ = difference, differential
η = cumulative number distribution of overvolumed crystals
μ_j = jth moment with respect to crystal volume, no.·m^{3j}/L
ρ_c = crystal density, kg/L
σ = relative supersaturation, $=(c-c^*)/c^*$
τ = mean residence time, s

Superscripts

$-$ = average

Literature Cited

David, R., P. Marchal, J. Villermaux, and J. P. Klein, "Crystallization and Precipitation Engineering: III. Discrete Formulation of the Agglomeration Rate of Crystals in a Crystallization Process," *Chem. Eng. Sci.*, **46**, 205 (1991a).

David, R., J. Villermaux, P. Marchal, and J. P. Klein, "Crystallization and Precipitation Engineering: IV. Kinetic Model of Adipic Acid Crystallization," *Chem. Eng. Sci.*, **46**, 1129 (1991b).

Delpech de Saint Guilhem, X., and T. A. Ring, "Exact Solution for the Population in a Countinuous Stirred Tank Crystallizer with Agglomeration," *Chem. Eng. Sci.*, **42**, 1247 (1987).

Drake, R. L., "A General Mathematical Survey of the Coagulation Equation," *Topics in Current Aerosol Research*, Part 2, G. M. Hidy and J. R. Brock, eds., Pergamon Press, New York (1972).

Franck, R., R. David, J. Villermaux, and J. P. Klein, "Crystallization and Precipitation Engineering: II. a Chemical Reaction Engineering Approach to Salicylic Acid Precipitation: Modelling of Batch Kinetics and Application to Continuous Operation," *Chem. Eng. Sci.*, **43**, 69 (1988).

Grabenbauer, G. C., and C. E. Glatz, "Protein Precipitation—Analysis of Particle Size Distribution and Kinetics," *Chem. Eng. Commun.*, **12**, 203 (1981).

Hartel, R. W., B. E. Gottung, A. D. Randolph, and G. W. Drach, "Mechanisms and Kinetic Modeling of Calcium Oxalate Crystal Aggregation in a Urinelike Liquor: I. Mechanisms," *AIChE J.*, **32**(7), 1176 (1986).

Hartel, R. W., and A. D. Randolph, "Mechanisms and Kinetic Modeling of Calcium Oxalate Crystal Aggregation in a Urinelike Liquor: II. Kinetic Modeling," *AIChE J.*, **32**(7), 1186 (1986).

Hounslow, M. J., R. L. Ryall, and V. R. Marshall, "A Discretized Population Balance for Nucleation, Growth, and Aggregation," *AIChE J.*, **34**(11), 1821 (1988).

Hounslow, M. J., "A Discretized Population Balance for Continuous Systems at Steady State," *AIChE J.*, **36**(1), 106 (1990a).

Hounslow, M. J., "Nucleation, Growth and Aggregation Rates From Steady State Experimental Data," *AIChE J.*, **36**(11), 1748 (1990b).

Hulburt, H. M., and S. Katz, "Some Problems in Particle Technology: a Statistical Mechanical Formulation," *Chem. Eng. Sci.*, **19**, 555 (1964).

Lamey, M. D., and T. A. Ring, "The Effects of Agglomeration in a Continuous Stirred Tank Crystallizer," *Chem. Eng. Sci.*, **41**, 1213 (1986).

Liao, P. F., and H. M. Hulburt, "Agglomeration Processes in Suspension Crystallization," AIChE Meeting, Chicago (Dec. 1976).

Marchal, P., R. David, J. P. Klein, and J. Villermaux, "Crystallization and Precipitation Engineering: I. an Efficient Method for Solving Population Balance in Crystallization with Agglomeration," *Chem. Eng. Sci.*, **43**(1), 59 (1988).

Masy, J. C., and M. Cournil, "Using a Turbidimetric Method to Study the Kinetics of Agglomeration of Potassium Sulphate in a Liquid Medium," *Chem. Eng. Sci.*, **46**, 693 (1991).

Przybycien, T. M., and J. E. Bailey, "Aggregation Kinetics in Salt Induced Protein Precipitation," *AIChE J.*, **35**(11), 1779 (1989).

Randolph, A. D., and M. D. Cise, "Nucleation Kinetics of the Potassium Sulfate—Water System," *AIChE J.*, **18**, 798 (1972).

Rosen, H. N., and H. M. Hulburt, "Continuous Vacuum Crystallization of Potassium Sulphate," *AIChE Symp. Ser.*, **67**(110), 18 (1971).

Tavare, N. S., and J. Garside, "Simultaneous Estimation of Crystal Nucleation and Growth Kinetics from Batch Experiments," *Chem. Eng. Res. Des.*, **64**(2), 109 (1986).

Tavare, N. S., M. B. Shah, and J. Garside, "Crystallization and Agglomeration Kinetics of Nickel Ammonium Sulphate in an MSMPR Crystallizer," *Powder Technol.*, **44**, 13 (1985).

Tavare, N. S., "Mixing in Continuous Crystallizers," *AIChE J.*, **32**(5), 705 (1986).

Tavare, N. S., Letter to the Editor, *AIChE J.*, **37**, 792 (1991).

Youngquist, G. R., and A. D. Randolph, "Secondary Nucleation in a Class II System: Ammonium Sulfate-Water," *AIChE J.*, **18**, 421 (1972).

Zumstein, R. C., and R. W. Rousseau, "Agglomeration of Copper Sulphate Pentahydrate Crystals within Well-Mixed Crystallizers," *Chem. Eng. Sci.*, **44**(10), 2149 (1989a).

Zumstein, R. C., and R. W. Rousseau, "Anomalous Growth of Large and Small Copper Sulphate Pentahydrate Crystals," *Ind. Eng. Chem. Res.*, **28**, 289 (1989b).

Manuscript received Aug. 7, 1991, and revision received Dec. 18, 1991.